

LETTER TO THE EDITOR

Sub-Poissonian photon statistics of higher harmonics: quantum predictions via classical trajectories

Jiří Bajér† and Adam Miranowicz‡§

† Department of Optics, Palacký University, 17. listopadu 50, 772 00 Olomouc, Czech Republic

‡ Department of Information Science, Kochi University, Kochi 780-8520, Japan

§ Nonlinear Optics Division, Institute of Physics, Adam Mickiewicz University, 61-614 Poznań, Poland

Received 24 January 2000

Abstract. Second-harmonic generation in the no-energy-transfer regime can be a source of quasi-stationary sub-Poissonian light as was recently shown by Bajér *et al* (Bajér J, Haderka O and Peřina J 1999 *J. Opt. B: Quantum Semiclass. Opt.* **1** 529). We generalize their results for higher-harmonic generation by applying the numerical method of Hamiltonian diagonalization and the analytical semiclassical description of classical trajectories. The quasi-stationary behaviour of the sub-Poissonian photocount noise in the no-energy-transfer regime is explained. An approximate formula for the Fano factor is derived for arbitrary harmonics. It is predicted that the deepest quasi-stationary reduction of photocount noise in the no-energy-transfer regime is achieved in the third-harmonic generation.

Keywords: Photon statistics, sub-Poissonian statistics, harmonic generation, classical trajectories

1. Introduction

Second-harmonic generation has attracted considerable interest as a candidate to generate nonclassical radiation (see [1, 2] for a detailed account and bibliography). It was demonstrated, in particular, that the photon antibunched, sub-Poissonian [3], squeezed [4] and generalized squeezed [5, 6] light can be generated in this process. In experimental schemes, second-harmonic generation is usually applied for the sub-Poissonian and photon-antibunched light production, whereas second-subharmonic generation (also referred to as two-photon down conversion) is used for the squeezed-light generation [1, 7]. Non-classical effects in higher-harmonic generation have also been investigated, including sub-Poissonian photocount statistics [2, 8–10], ordinary squeezing [2, 11, 12], higher-order squeezing [13, 15] according to the Hong–Mandel definition [5] and higher-power-amplitude squeezing [14, 15] based on Hillery’s concept [6].

We will study photocount statistics of N th-harmonic generation processes. Photocount noise of the observed statistics can simply be described by the (quantum) *Fano factor*

$$F = \frac{\text{Var}(n)}{\langle n \rangle}, \quad (1)$$

where $\langle n \rangle$ represents the mean number of detected photons and $\text{Var}(n) = \langle n^2 \rangle - \langle n \rangle^2$ is the variance of photon number. For $F < 1$, the light is referred to as sub-Poissonian since it has photocount noise smaller than that of coherent (ideal laser) light with the same intensity. Whereas for $F > 1$, the light is called super-Poissonian exhibiting photocount noise higher than the coherent-light noise.

Processes of the N th-harmonic or subharmonic generation can be described by the conventional interaction Hamiltonian (e.g., [2])

$$H = \hbar g (a_1^N a_N^\dagger + a_1^\dagger a_N) \quad (2)$$

for $N = 2, 3, \dots$. In (2), a_1 and a_N denote annihilation operators of the fundamental and N th-harmonic modes, respectively, and g is a nonlinear coupling parameter.

Investigations of non-classical effects in harmonic generation have usually been restricted to the regime of short interactions (short optical paths, short times, or short lengths). Theoretical predictions of quantum parameters (including the Fano F -factor or, equivalently, the Mandel Q -parameter) were obtained under the short-time approximation only (see, e.g., [1, 2, 10]). This approximation is usually valid due to a weak nonlinear coupling of the optical fields.

In a recent paper, Bajér *et al* [17] studied numerically second-harmonic generation in a long-interaction regime.

On testing different coherent input amplitudes in order to minimize the Fano factor, they discovered a previously unknown special regime yielding the long-interaction output with the quasi-stationary sub-Poissonian photocount noise. The regime occurs if the ratio of the amplitudes α_1 and α_N is equal to N , i.e., if the initial coherent vectors are given by $|\alpha_1\rangle = |Nr\rangle$ and $|\alpha_N\rangle = |r\rangle$. This is a quantum analogue of the so-called *no-energy-transfer regime* [18] known in classical nonlinear optics as an evolution exhibiting no energy transfer between the interacting modes, which occurs if the initial amplitudes and phases fulfil the conditions $r_1 = Nr_N$ and $N\phi_1 = \phi_N$, respectively. The intensities of both modes remain quasi-constant in time during the interaction. Obviously, in a quantum description some small energy fluctuations between modes are observed as a consequence of vacuum fluctuations. However, the influence of energy fluctuations can be neglected for strong fields.

Bajer *et al* [17] also applied the approximate method of classical trajectories to explain time stability of the solutions, and compared with numerical predictions of the photocount noise. In particular, the quasi-stationary behaviour of the second harmonic in the no-energy-transfer regime was described by the semiclassical Fano factor $F_2 = \frac{5}{6} \approx 0.83$ and tested to be in a good agreement with the numerical value of the quantum Fano factor.

In this letter, we generalize for N th-harmonic generation, the numerical and analytical results derived in [17] for the special case of $N = 2$. We will show, as our main result, that higher-harmonic generation in the no-energy-transfer regime can serve as a source of the quasi-stationary sub-Poissonian light. We will derive a formula for the semiclassical Fano factor having its minimum of $F_N = 0.81$ at $N = 3$. Thus, we conclude that quasi-stationary light with the most suppressed photocount noise in the no-energy-transfer regime is produced in the process of third-harmonic generation.

2. Classical trajectory analysis

The complete quantum solution of the model given by Hamiltonian (2) can only be found by applying sophisticated numeric methods on a fast computer. However, since we are interested in a special type of solution for strong fields we can adopt approximate methods of, e.g., classical trajectories [19] and obtain some analytical results. The method adequately simulates quantum noise for various nonlinear optical processes if the initial conditions are properly chosen to describe the quantum noise of coherent states. Along the lines of the classical trajectory method, we choose initial amplitudes $\alpha = a$ and blur them with Gaussian noise, which results in $\alpha = a + x + iy$, where x and y are real Gaussian stochastic quantities with the identical variances $\sigma^2 = \frac{1}{4}$. In this case, we get correct quantities for the quantum noise parameters including the semiclassical squeezing variance

$$S^{cl} = \text{Var}(X) = \text{Var}(\alpha e^{-i\theta} + \alpha^* e^{i\theta}) = 4\sigma^2 = 1 \quad (3)$$

and the semiclassical Fano factor

$$F^{cl} = \frac{\overline{\alpha^* \alpha^2} - \overline{\alpha^* \alpha}^2}{\overline{\alpha^* \alpha}} = \frac{4\sigma^2(a^2 + \sigma^2)}{a^2 + 2\sigma^2} = \frac{a^2 + \frac{1}{4}}{a^2 + \frac{1}{2}} \rightarrow 1. \quad (4)$$

We assume strong initial fields (i.e. $a \gg 1$). As will explicitly be demonstrated, this classical description of quantum noise breaks down for weak fields ($a < 1$). To calculate statistical moments, including the Fano factor (4) or the squeezing variance (3), one needs to solve the classical evolution for each process separately and then, to average the analysed statistical moments over all obtained trajectories.

The semiclassical process of the N th-harmonic generation can be described by the pair of complex differential equations [20]

$$\begin{aligned} \dot{\alpha}_1 &= -igN\alpha_1^{*N-1}\alpha_N, \\ \dot{\alpha}_N &= -ig\alpha_1^N. \end{aligned} \quad (5)$$

On introducing real amplitudes and phases, $\alpha_k = r_k e^{i\phi_k}$, (5) can be transformed into the system of three real equations:

$$\begin{aligned} \dot{r}_1 &= -gNr_1^{N-1}r_N \sin \theta, \\ \dot{r}_N &= gr_1^N \sin \theta, \\ \dot{\theta} &= g \left(\frac{r_1^N}{r_N} - N^2 r_1^{N-2} r_N \right) \cos \theta, \end{aligned} \quad (6)$$

where $\theta = N\phi_1 - \phi_N$ is the phase mismatch. Equations (6) have two integrals of motion:

$$\begin{aligned} E &= r_1^2 + Nr_N^2 = n_1 + Nn_N, \\ \Gamma &= r_1^N r_N \cos \theta. \end{aligned} \quad (7)$$

On extraction of r_1 and θ from (6), we find an equation for the amplitude r_N :

$$(r_N \dot{r}_N / g)^2 + \Gamma^2 = r_N^2 (E - Nr_N^2)^N \quad (8)$$

or its simpler form for the intensity $n_N = r_N^2$:

$$\left(\frac{\dot{n}_N}{2g} \right)^2 = n_N (E - Nn_N)^N - \Gamma^2. \quad (9)$$

The general solution for $n_N(t)$ is a periodic function oscillating between the values n_{\min} and n_{\max} . For $N = 2$ and 3, the solution is given in terms of the Jacobi elliptical functions.

The only elementary solution of (6) is obtained for the vanishing initial phase mismatch ($\theta = 0$) and the initial amplitudes satisfying the condition $r_1 = Nr_N$. The solution reads as

$$\begin{aligned} \alpha_1(t) &= r_1 \exp(-igt r_1^{N-1} + i\varphi), \\ \alpha_N(t) &= r_N \exp[N(-igt r_1^{N-1} + i\varphi)] \end{aligned} \quad (10)$$

and has a form of the so-called no-energy-transfer solution, since the amplitude and energy in both the interacting modes remain constant $n_1(t) = |\alpha_1(t)|^2 = r_1^2$ and $n_N(t) = |\alpha_N(t)|^2 = r_N^2$ [18]. We will use the method of classical trajectories along the lines of the analysis presented in [17]. We solve a large set of separated processes described by (5), where input amplitudes fulfil the conditions for the no-energy-transfer case. We choose initial amplitudes $\alpha_1 = Nr$

and $\alpha_N = r$, and blur them with Gaussian noise, which results in

$$\begin{aligned}\alpha_1 &= Nr + x_1 + iy_1, \\ \alpha_N &= r + x_N + iy_N,\end{aligned}\quad (11)$$

where x_k and y_k are real and mutually independent Gaussian stochastic quantities with the identical variances $\sigma^2 = \frac{1}{4}$. We assume strong initial fields, i.e. $r \gg 1$. The integrals of motion, given by (7), can be expressed in a form of corrections in successive powers of r :

$$E = N(N+1)r^2 + \Delta E_1 + \Delta E_0, \quad (12)$$

where

$$\begin{aligned}\Delta E_1 &= 2N(x_1 + x_N)r, \\ \Delta E_0 &= x_1^2 + y_1^2 + N(x_N^2 + y_N^2),\end{aligned}\quad (13)$$

and

$$\Gamma = N^N r^{N+1} + \Delta\Gamma_N + \Delta\Gamma_{N-1} + \Delta\Gamma_{N-2} + \dots, \quad (14)$$

where

$$\begin{aligned}\Delta\Gamma_N &= N^N (x_1 + x_N)r^N, \\ \Delta\Gamma_{N-1} &= \left[\frac{N-1}{2}(x_1^2 - y_1^2) + N(x_1x_N + y_1y_N) \right] \\ &\quad \times N^{N-1}r^{N-1}.\end{aligned}\quad (15)$$

The lower-order terms $\Delta\Gamma_{N-2}, \Delta\Gamma_{N-3}, \dots$ can be neglected in further considerations. On assumption of strong interacting fields ($r \gg 1$), we substitute

$$n_N = \frac{E}{N(N+1)} + \epsilon, \quad (16)$$

where ϵ is a small correction of stationary value. Then, (9) can be rewritten as

$$\begin{aligned}\left(\frac{\dot{n}_N}{2g}\right)^2 &= n_N(E - Nn_N)^N - \Gamma^2 \\ &\approx \frac{N^{N-1}}{(N+1)^{N+1}}E^{N+1} - \frac{N^N}{2(N+1)^{N-2}}E^{N-1}\epsilon^2 - \Gamma^2 \\ &= \frac{N^N}{2(N+1)^{N-2}}E^{N-1}(A^2 - \epsilon^2)\end{aligned}\quad (17)$$

on omission of higher-order terms involving $\epsilon^3, \epsilon^4, \dots$. One arrives at the simple equation

$$\left(\frac{\dot{\epsilon}}{2g}\right)^2 = \frac{N^N}{2(N+1)^{N-2}}E^{N-1}(A^2 - \epsilon^2). \quad (18)$$

Thus, the solution of (9) reads as

$$\begin{aligned}n_N(t) &= \frac{E}{N(N+1)} + A \sin(\Omega gt + \varphi) \\ &= r^2 + B + A \sin(\Omega gt + \varphi),\end{aligned}\quad (19)$$

where frequency Ω is given by

$$\Omega = \sqrt{\frac{2N^N E^{N-1}}{(N+1)^{N-2}}} \quad (20)$$

and

$$\begin{aligned}A &= \frac{r}{N+1} \sqrt{4(x_1 - Nx_N)^2 + 2N(N+1)(y_1 - y_N)^2} \\ B &= \frac{\Delta E_1}{N(N+1)} = \frac{2}{N+1}r(x_1 + x_N).\end{aligned}\quad (21)$$

The phase correction φ can be derived from the equation $n_N(0) \approx 2rx_N = B + A \sin \varphi$. From (7), a result similar to (19) is obtained for the fundamental mode:

$$\begin{aligned}n_1(t) &= E - Nn_N(t) \\ &= N^2r^2 + N^2B - NA \sin(\Omega gt + \varphi).\end{aligned}\quad (22)$$

It is seen that both solutions (19) and (22) are given in a form of large constants weakly perturbed by harmonic functions. Now, on applying the classical trajectory method, one should perform averaging over all solutions (19) and (22) to calculate the required statistical moments. Here, we calculate the first- and second-order field-intensity moments necessary for determination of the Fano factors. The mean intensities of the fundamental and harmonic modes are simply given by $\bar{n}_1 = N^2r^2$ and $\bar{n}_N = r^2$, respectively. The second-order moments of field intensity are found to be

$$\begin{aligned}\bar{n}_1^2 &= N^4r^4 + N^4\bar{B}^2 + \frac{1}{2}N^2\bar{A}^2, \\ \bar{n}_N^2 &= r^4 + \bar{B}^2 + \frac{1}{2}\bar{A}^2.\end{aligned}\quad (23)$$

in terms of $\bar{A}^2 = r^2(2N^2 + N + 1)(N + 1)^{-2}$ and $\bar{B}^2 = 2r^2(N + 1)^{-2}$. We note that \bar{B} vanishes. The term $\sin^2(\Omega gt + \varphi)$ can simply be estimated as $\frac{1}{2}$ for sufficiently long time t , when n and F become time independent. Relaxation in $n_k(t)$ and $F_k(t)$ is observed for short times t due to the presence of the harmonic sine function. The mean value of the frequency (20), given by

$$\bar{\Omega} \approx \sqrt{2N(N+1)}(Nr)^{N-1}, \quad (24)$$

enables estimation of the oscillation period $T_{\text{osc}} = 2\pi/\bar{\Omega}$, whereas the standard deviation

$$\Delta\Omega \approx \sqrt{2N(N+1)}N^{N-1}r^{N-2} \frac{N-1}{N+1} \quad (25)$$

determines the duration $T_{\text{rel}} = 2\pi/\Delta\Omega$ of relaxation. By comparing the characteristic times T_{osc} and T_{rel} , one finds that the evolution time can be scaled by $\tau = \bar{\Omega}gt$ to synchronize optimally the oscillations of the exact quantum solutions for different N . These synchronized oscillations of the Fano factors are clearly presented in figures 1(a) and (b).

Finally, we arrive at the semiclassical Fano factors

$$F_1^{cl} = \frac{\bar{n}_1^2 - \bar{n}_1}{\bar{n}_1} = \frac{1}{2} \frac{6N^2 + N + 1}{(N+1)^2}, \quad (26)$$

$$F_N^{cl} = \frac{\bar{n}_N^2 - \bar{n}_N}{\bar{n}_N} = \frac{1}{2} \frac{2N^2 + N + 5}{(N+1)^2}, \quad (27)$$

which are the compact-form classical analogues of the quantum Fano factors. The semiclassical Fano factors for the fundamental and higher harmonics for various values of N are listed in tables 1 and 2, and plotted in figures 2(a) and (b), respectively.

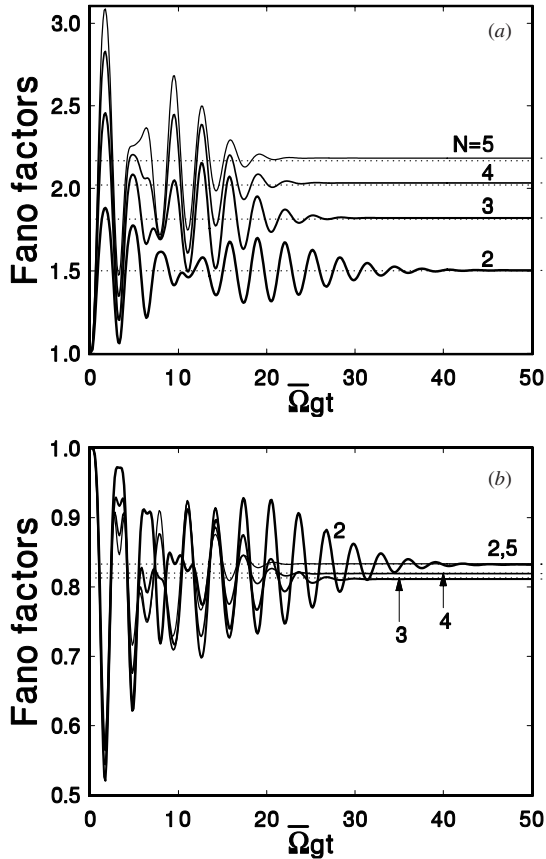


Figure 1. Time evolution of the exact quantum Fano factors: (a) $F_1 = F_1(N)$ for the fundamental mode and (b) F_N for the harmonic mode in N th-harmonic generation for $N=2$ (thickest curve), 3, 4, 5 (thinnest curve). Time t is rescaled with frequency $\bar{\Omega}$, given by (24), and coupling constant g . The harmonic-mode amplitude is $r = r_N = 5$. The dotted lines represent the semiclassical Fano factors, given by (26) and (27). It is seen that the fundamental mode is super-Poissonian, whereas the harmonic mode is sub-Poissonian for all non-zero evolution times.

Table 1. Quasi-stationary values of the quantum Fano factors F_1 and their semiclassical approximations F_1^{cl} , given by (26), for the fundamental mode in N th-harmonic generation with $N = 1-5$ in the no-energy-transfer regime. The values of F_1 are calculated for $r = r_N = 5$.

N	F_1	F_1^{cl}	$(F_1 - F_1^{cl})/F_1$
1	1	1	0
2	1.502 9291	$\frac{3}{2}$	0.0020
3	1.820 2032	$\frac{29}{16}$	0.0042
4	2.032 3293	$\frac{101}{50}$	0.0061
5	2.183 0414	$\frac{13}{6}$	0.0075

Our solutions (26) and (27) for $N = 2$ reduce to the results derived in [17]. By analysing (27), we find that the higher harmonics evolve into quasi-stationary sub-Poissonian states ($F_N^{cl} < 1$) for any $N > 1$. Except for the second harmonic, the photocount noise reduction in the higher harmonics becomes less effective with increasing N . Thus, the deepest noise reduction occurs for the third harmonic as described by the Fano factor $F_3^{cl} = \frac{13}{16} = 0.8125$. The photocount noise reductions for the second

Table 2. Same as in table 1, but for the N th-harmonic mode; F_N^{cl} are calculated from (27).

N	F_N	F_N^{cl}	$ F_N - F_N^{cl} /F_N$
1	1	1	0
2	0.832 288 00	$\frac{5}{6}$	0.001 3
3	0.811 259 70	$\frac{13}{16}$	0.001 5
4	0.819 249 02	$\frac{41}{50}$	0.000 92
5	0.833 311 27	$\frac{5}{6}$	0.000 026

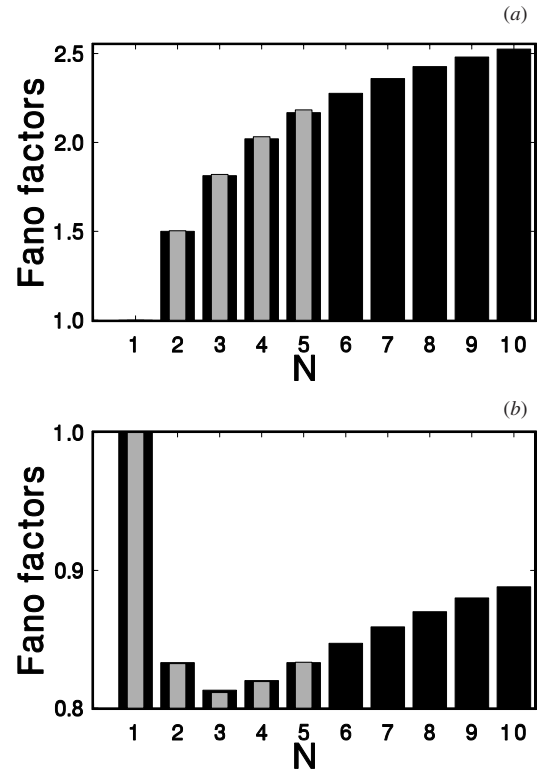


Figure 2. Semiclassical (solid bars) and quantum (dithered bars) Fano factors versus order N of harmonic generation for (a) fundamental and (b) N th-harmonic modes in the quasi-stationary no-energy-transfer regime. (a) and (b) for $N = 1-5$ correspond to tables 1 and 2, respectively. It is seen that the quantum results are well fitted by the semiclassical Fano factors. According to both descriptions, the third-harmonic mode has the most suppressed photocount noise.

and fifth harmonics are predicted to be the same, although the quantum analysis (see table 2) reveals that they differ slightly ($< 1\%$). As given by (26), the fundamental mode has solely the super-Poissonian photocount statistics ($F_1^{cl} > 1$) with noise monotonically growing in N for the no-energy-transfer regime. For $N = 1$ the process is linear and no change in the photon statistics occurs. The interacting modes remain coherent with unit Fano factors for both modes. It is worth noting that qualitatively different photocount statistics of the fundamental mode are observed in the short-interaction regime. In this case, Kozierowski and Tanaś [3] showed that the output light, both at the second harmonic and fundamental frequencies, has the sub-Poissonian photocount statistics.

3. Quantum analysis

In order to test the validity of our semiclassical results, we give an exact quantum analysis of N th-harmonic generation on applying a numerical method of the Hamiltonian diagonalization proposed by Walls and Barakat [16]. The method can be applied for arbitrary initial photon statistics. Nevertheless, for the purpose of this letter, we restrict our analysis solely to the initial coherent fields. Due to the obvious computational difficulties, the results can be obtained only for small numbers of interacting photons. The analysis of about 100 interacting photons practically reaches our computational capabilities.

For better comparison of theoretical predictions for different order processes, we have plotted in figure 1 the quantum Fano factors for both interacting modes in the no-energy-transfer regime with $N = 2-5$ and $r = 5$. One can see that all the curves start from $F_{1,N}(0) = 1$ for the input coherent fields and become quasi-stationary after some relaxations. The quantum and semiclassical Fano factors coincide for high-intensity fields and longer times ($t \sim 50/(\Omega g)$).

All fundamental modes remain super-Poissonian $F_1(t) > 1$, whereas the N th harmonics become sub-Poissonian $F_N(t) < 1$. The most suppressed noise is observed for the third harmonic with the Fano factor $F_3 \approx 0.81$. In figure 1, we have included the predictions of the classical trajectory method (plotted as dotted lines) to show that they properly fit the exact quantum results for the evolution times $t \sim 50/(\Omega g)$. The small residual differences result from the fact that the amplitude r was chosen to be relatively small ($r = 5$). This value does not precisely fulfil the condition $r \gg 1$. We have taken $r = 5$ as a compromise between the asymptotic value $r \rightarrow \infty$ and computational complexity to manipulate the matrices of dimensions 1000×1000 . Unfortunately, we cannot increase amplitude r arbitrarily due to serious computational difficulties.

The numerical values of the quantum Fano factors in comparison with their semiclassical approximations for the fundamental mode, given by (26), are presented in their dependence on N in table 1 and figure 2(a). Analogously, those values for harmonics are presented in figure 2(b) and table 2 as calculated by the numerical quantum method and from analytical semiclassical formula (27). It is seen that the approximate predictions of the Fano factors according to (26) and (27) fit very well the values obtained on applying the numerical quantum method. Actually, the differences between the approximate and exact values are hardly visible on the scale of figure 2. Nevertheless, some small (<1%) differences in $F_{1,N}$ (see tables 1 and 2) can be explained by the fact that the value of r for numerical analysis was chosen too small.

We have shown, in agreement with the results presented in [17], that the method of classical trajectories gives very good predictions in the case of strong-field interactions (i.e. for photon numbers much larger than 1). The calculation speed of the method does not depend on the number of interacting photons. However, better approximation is achieved with increasing number of photons. Thus, the

method is very fast and significantly simplifies the tedious exact quantum calculations.

4. Conclusions

We have analysed N th-harmonic generation processes as a generalization of the results for $N = 2$ derived in [17]. We have shown numerically in a quantum description that the fundamental and N th-harmonic modes evolve into quasi-stationary states in the no-energy-transfer regime. Good analytical predictions of the Fano factors for both the fundamental and harmonic modes were obtained under the semiclassical approximation in the strong-field limit. Quantum analysis has completely confirmed our predictions derived via classical trajectories. The fundamental mode evolves into a quasi-stationary state with the super-Poissonian ($F_1 > 1$) photocount statistics, whereas the N th harmonic goes over into a sub-Poissonian ($F_N < 1$) quasi-stationary state. We have found that the most suppressed photocount noise is obtained for the third harmonic as described by the Fano factor $F_3 = 0.81$.

JB thanks the Czech Ministry of Education for support under grants VS96028 and CEZ J14/98 and the Grant Agency of the Czech Republic 202/00/0142. AM is indebted to Professor Hideaki Matsueda for his hospitality and stimulating research at Kochi University. AM also gratefully acknowledges a scholarship from the Japanese Ministry of Education (Monbusho).

References

- [1] Mandel L and Wolf E 1995 *Optical Coherence and Quantum Optics* (Cambridge: Cambridge University Press) sections 12.10 and 14.9
- [2] Peřina J 1991 *Quantum Statistics of Linear and Nonlinear Optical Phenomena* (Dordrecht: Kluwer) ch 10
- [3] Kozierowski M and Tanař R 1977 *Opt. Commun.* **21** 229
- [4] Mandel L 1982 *Opt. Commun.* **42** 437
- [5] Hong C K and Mandel L 1982 *Phys. Rev. A* **32** 974
- [6] Hillery M 1987 *Opt. Commun.* **62** 135
- [7] Peřina J, Hradil Z and Jurčo B 1994 *Quantum Optics and Fundamentals of Physics* (Dordrecht: Kluwer) ch 8.5
Bachor H A 1998 *A Guide to Experiments in Quantum Optics* (Weinheim: Wiley-VCH) ch 9
- [8] Kielich S, Kozierowski M and Tanař R 1978 *Coherence and Quantum Optics* vol 4, ed L Mandel and E Wolf (New York: Plenum) p 511
- [9] Malakyan Y P 1991 *Opt. Commun.* **86** 423
- [10] Bajer J and Peřina J 1992 *Opt. Commun.* **92** 99
- [11] Kozierowski M and Kielich S 1983 *Phys. Lett.* **94** 213
- [12] Bajer J, Opatrný T and Peřina J 1994 *Quantum Opt.* **6** 403
- [13] Kozierowski M 1986 *Phys. Rev. A* **34** 3474
- [14] Zhan Y B 1992 *Phys. Rev. A* **46** 686
- [15] Du S D and Gong C D 1993 *Phys. Rev. A* **48** 2198
- [16] Walls D and Barakat R 1970 *Phys. Rev. A* **1** 446
- [17] Bajer J, Haderka O and Peřina J 1999 *J. Opt. B: Quantum Semiclass. Opt.* **1** 529
- [18] Paul H 1973 *Nichtlineare Optik* vol 2 (Berlin: Akademie) p 16
Bandilla A, Drobný G and Jex I 1996 *Opt. Commun.* **128** 353
Drobný G, Bandilla A and Jex I 1997 *Phys. Rev. A* **55** 78
- [19] Nikitin S P and Masalov A V 1991 *Quantum Opt.* **3** 105
Milburn G J 1986 *Phys. Rev. A* **33** 674
- [20] Boyd R W 1991 *Nonlinear Optics* (New York: Academic) p 78
Bandilla A, Drobný G and Jex I 1998 *Opt. Commun.* **156** 112